

# 12

## Variational Formulation of Plane Beam Element

## TABLE OF CONTENTS

	Page
<b>§12.1 Introduction</b> . . . . .	12–3
<b>§12.2 What is a Beam?</b> . . . . .	12–3
§12.2.1 Terminology . . . . .	12–3
§12.2.2 Mathematical Models . . . . .	12–3
§12.2.3 Assumptions of Classical Beam Theory . . . . .	12–4
<b>§12.3 The Bernoulli-Euler Beam Theory</b> . . . . .	12–4
§12.3.1 Element Coordinate Systems . . . . .	12–4
§12.3.2 Kinematics . . . . .	12–5
§12.3.3 Loading . . . . .	12–5
§12.3.4 Support Conditions . . . . .	12–5
§12.3.5 Strains, Stresses and Bending Moments . . . . .	12–5
<b>§12.4 Total Potential Energy Functional</b> . . . . .	12–6
<b>§12.5 Beam Finite Elements</b> . . . . .	12–7
§12.5.1 Finite Element Trial Functions . . . . .	12–8
§12.5.2 Shape Functions . . . . .	12–8
<b>§12.6 The Finite Element Equations</b> . . . . .	12–9
§12.6.1 The Stiffness Matrix of a Prismatic Beam . . . . .	12–10
§12.6.2 Consistent Nodal Force Vector for Uniform Load . . . . .	12–11
<b>§12. Notes and Bibliography</b> . . . . .	12–15
<b>§12. References</b> . . . . .	12–15
<b>§12. Exercises</b> . . . . .	12–16

### §12.1. Introduction

The previous Chapter introduced the TPE-based variational formulation of finite elements, which was illustrated for the bar element. This Chapter applies that technique to a more complicated one-dimensional element: the plane beam described by engineering beam theory.

Mathematically, the main difference of beams with respect to bars is the increased order of continuity required for the assumed transverse-displacement functions to be admissible. Not only must these functions be continuous but they must possess continuous  $x$  first derivatives. To meet this requirement both deflections *and* slopes are matched at nodal points. Slopes may be viewed as *rotational* degrees of freedom in the small-displacement assumptions used here.

### §12.2. What is a Beam?

Beams are the most common type of structural component, particularly in Civil and Mechanical Engineering. A *beam* is a bar-like structural member whose primary function is to support *transverse loading* and carry it to the supports. See Figure 12.1.

By “bar-like” it is meant that one of the dimensions is considerably larger than the other two. This dimension is called the *longitudinal dimension* or *beam axis*. The intersection of planes normal to the longitudinal dimension with the beam member are called *cross sections*. A *longitudinal plane* is one that passes through the beam axis.

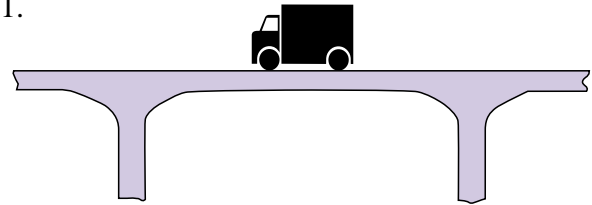


FIGURE 12.1. A beam is a structural member designed to resist transverse loads.

A beam resists transverse loads mainly through *bending action*. Bending produces compressive longitudinal stresses in one side of the beam and tensile stresses in the other.

The two regions are separated by a *neutral surface* of zero stress. The combination of tensile and compressive stresses produces an internal *bending moment*. This moment is the primary mechanism that transports loads to the supports. The mechanism is illustrated in Figure 12.2.

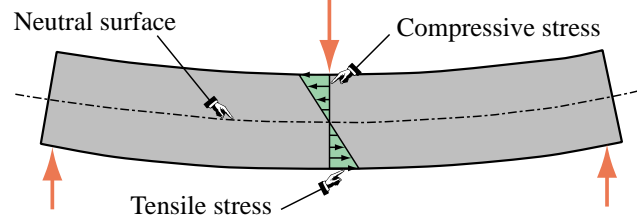


FIGURE 12.2. Beam transverse loads are primarily resisted by bending action.

#### §12.2.1. Terminology

A *general beam* is a bar-like member designed to resist a combination of loading actions such as biaxial bending, transverse shears, axial stretching or compression, and possibly torsion. If the internal axial force is compressive, the beam has also to be designed to resist buckling. If the beam is subject primarily to bending and axial forces, it is called a *beam-column*. If it is subjected primarily to bending forces, it is called simply a beam. A beam is *straight* if its longitudinal axis is straight. It is *prismatic* if its cross section is constant.

A *spatial beam* supports transverse loads that can act on arbitrary directions along the cross section. A *plane beam* resists primarily transverse loading on a preferred longitudinal plane. This Chapter considers only plane beams.

### §12.2.2. Mathematical Models

One-dimensional mathematical models of structural beams are constructed on the basis of *beam theories*. Because beams are actually three-dimensional bodies, all models necessarily involve some form of approximation to the underlying physics. The simplest and best known models for straight, prismatic beams are based on the *Bernoulli-Euler beam theory* (also called *classical beam theory* and *engineering beam theory*), and the *Timoshenko beam theory*. The Bernoulli-Euler theory is that taught in introductory Mechanics of Materials courses, and is the one emphasized in this Chapter. The Timoshenko beam model is presented in Chapter 13, which collects advanced material.

Both models can be used to formulate beam finite elements. The Bernoulli-Euler beam theory leads to the so-called *Hermitian* beam elements.<sup>1</sup> These are also known as  $C^1$  elements for the reason explained in §12.5.1. This model neglects the effect of transverse shear deformations on the internal energy. Elements based on Timoshenko beam theory, also known as  $C^0$  elements, incorporate a first order correction for transverse shear effects. This model assumes additional importance in dynamics and vibration.

### §12.2.3. Assumptions of Classical Beam Theory

The Bernoulli-Euler or classical beam theory for *plane beams* rests on the following assumptions:

1. *Planar symmetry*. The longitudinal axis is straight and the cross section of the beam has a longitudinal plane of symmetry. The resultant of the transverse loads acting on each section lies on that plane. The support conditions are also symmetric about this plane.
2. *Cross section variation*. The cross section is either constant or varies smoothly.
3. *Normality*. Plane sections originally normal to the longitudinal axis of the beam remain plane and normal to the deformed longitudinal axis upon bending.
4. *Strain energy*. The internal strain energy of the member accounts only for bending moment deformations. All other contributions, notably transverse shear and axial force, are ignored.
5. *Linearization*. Transverse deflections, rotations and deformations are considered so small that the assumptions of infinitesimal deformations apply.
6. *Material model*. The material is assumed to be elastic and isotropic. Heterogeneous beams fabricated with several isotropic materials, such as reinforced concrete, are not excluded.

## §12.3. The Bernoulli-Euler Beam Theory

### §12.3.1. Element Coordinate Systems

Under transverse loading one of the top surfaces shortens while the other elongates; see Figure 12.2. Therefore a *neutral surface* that undergoes no axial strain exists between the top and the bottom. The intersection of this surface with each cross section defines the *neutral axis* of that cross section.<sup>2</sup>

<sup>1</sup> The qualifier “Hermitian” relates to the use of a transverse-displacement interpolation formula studied by the French mathematician Hermite. The term has nothing to do with the mathematical model used.

<sup>2</sup> If the beam is homogenous, the neutral axis passes through the centroid of the cross section. If the beam is fabricated of different materials — for example, a reinforced concrete beam — the neutral axis passes through the centroid of an “equivalent” cross section. This topic is covered in Mechanics of Materials textbooks; for example Popov [595].

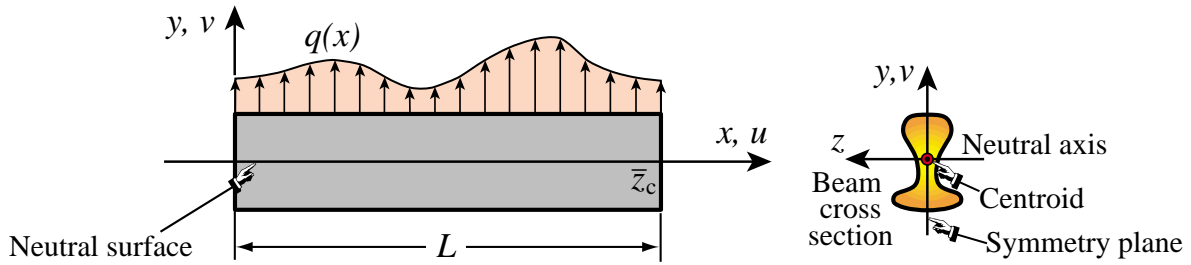


FIGURE 12.3. Terminology and choice of axes for Bernoulli-Euler model of plane beam.

The Cartesian axes for plane beam analysis are chosen as shown in Figure 12.3. Axis  $x$  lies along the longitudinal beam axis, at neutral axis height. Axis  $y$  lies in the symmetry plane and points upwards. Axis  $z$  is directed along the neutral axis, forming a RHS system with  $x$  and  $y$ . The origin is placed at the leftmost section. The total length (or span) of the beam member is called  $L$ .

### §12.3.2. Kinematics

The *motion* under loading of a plane beam member in the  $x, y$  plane is described by the two dimensional displacement field

$$\begin{bmatrix} u(x, y) \\ v(x, y) \end{bmatrix}, \quad (12.1)$$

where  $u$  and  $v$  are the axial and transverse displacement components, respectively, of an arbitrary beam material point. The motion in the  $z$  direction, which is primarily due to Poisson's ratio effects, is of no interest. The normality assumption of the Bernoulli-Euler model can be represented mathematically as

$$u(x, y) = -y \frac{\partial v(x)}{\partial x} = -y v' = -y \theta, \quad v(x, y) = v(x). \quad (12.2)$$

Note that the slope  $v' = \partial v / \partial x = dv / dx$  of the deflection curve has been identified with the *rotation* symbol  $\theta$ . This is permissible because  $\theta$  represents to first order, according to the kinematic assumptions of this model, the rotation of a cross section about  $z$  positive CCW.

### §12.3.3. Loading

The transverse force *per unit length* that acts on the beam in the  $+y$  direction is denoted by  $q(x)$ , as illustrated in Figure 12.3. Concentrated loads and moments acting on isolated beam sections can be represented by the delta function and its derivative. For example, if a transverse point load  $F$  acts at  $x = a$ , it contributes  $F\delta(a)$  to  $q(x)$ . If the concentrated moment  $C$  acts at  $x = b$ , positive CCW, it contributes  $C\delta'(b)$  to  $q(x)$ , where  $\delta'$  denotes a doublet acting at  $x = b$ .

### §12.3.4. Support Conditions

Support conditions for beams exhibit far more variety than for bar members. Two canonical cases are often encountered in engineering practice: simple support and cantilever support. These are illustrated in Figures 12.4 and 12.5, respectively. Beams often appear as components of skeletal structures called frameworks, in which case the support conditions are of more complex type.

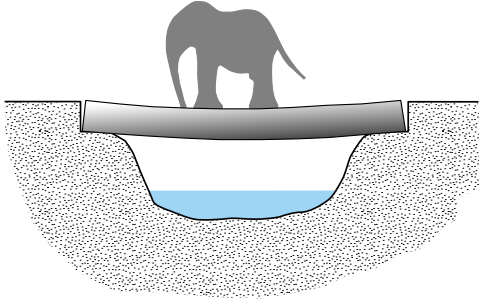


FIGURE 12.4. A simply supported beam has end supports that preclude transverse displacements but permit end rotations.

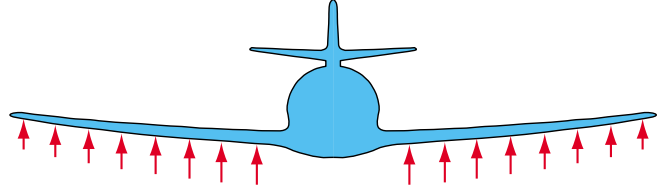


FIGURE 12.5. A cantilever beam is clamped at one end and free at the other. Airplane wings and stabilizers are examples of this configuration.

### §12.3.5. Strains, Stresses and Bending Moments

The Bernoulli-Euler or classical model assumes that the internal energy of beam member is entirely due to bending strains and stresses. Bending produces axial stresses  $\sigma_{xx}$ , which will be abbreviated to  $\sigma$ , and axial strains  $e_{xx}$ , which will be abbreviated to  $e$ . The strains can be linked to the displacements by differentiating the axial displacement  $u(x)$  of (12.2):

$$e = \frac{\partial u}{\partial x} = -y \frac{\partial^2 v}{\partial x^2} = -y \frac{d^2 v}{dx^2} = -y v'' = -y \kappa. \quad (12.3)$$

Here  $\kappa$  denotes the deformed beam axis curvature, which to first order is  $\kappa \approx d^2 v / dx^2 = v''$ . The bending stress  $\sigma = \sigma_{xx}$  is linked to  $e$  through the one-dimensional Hooke's law

$$\sigma = E e = -E y \frac{d^2 v}{dx^2} = -E y \kappa, \quad (12.4)$$

where  $E$  is the longitudinal elastic modulus. The most important stress resultant in classical beam theory is the *bending moment*  $M$ , which is defined as the cross section integral

$$M = \int_A -y \sigma dA = E \frac{d^2 v}{dx^2} \int_A y^2 dA = E I \kappa. \quad (12.5)$$

Here  $I \equiv I_{zz}$  denotes the moment of inertia  $\int_A y^2 dA$  of the cross section with respect to the  $z$  (neutral) axis. The bending moment  $M$  is considered positive if it compresses the upper portion:  $y > 0$ , of the beam cross section, as illustrated in Figure 12.6. This convention explains the negative sign of  $y$  in the integral (12.5). The product  $E I$  is called the *bending rigidity* of the beam with respect to flexure about the  $z$  axis.

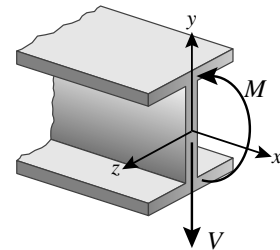


FIGURE 12.6. Positive sign convention for  $M$  and  $V$ .

The governing equations of the Bernoulli-Euler beam model are summarized in the Tonti diagram of Figure 12.7.

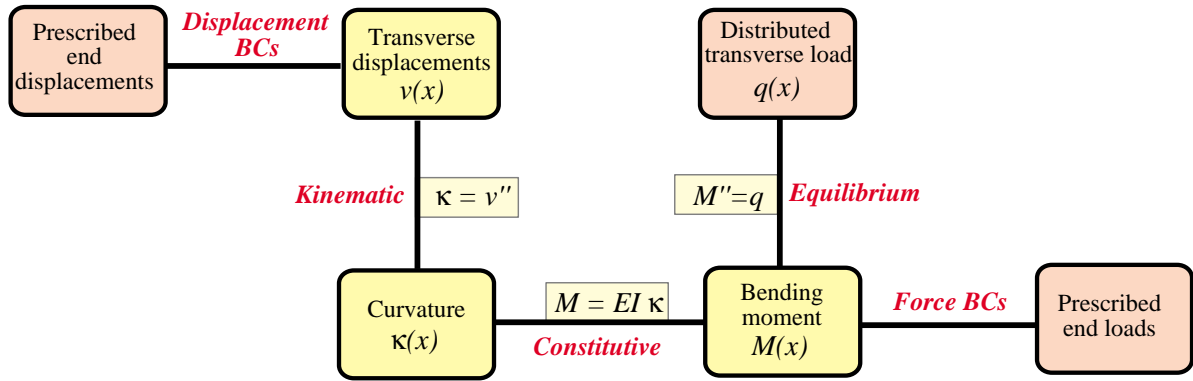


FIGURE 12.7. The Tonti diagram for the governing equations of the Bernoulli-Euler beam model.

### §12.4. Total Potential Energy Functional

The total potential energy of the beam is

$$\Pi = U - W \quad (12.6)$$

where as usual  $U$  and  $W$  denote the internal and external energies, respectively. As previously explained, in the Bernoulli-Euler model  $U$  includes only the bending energy:

$$U = \frac{1}{2} \int_V \sigma e \, dV = \frac{1}{2} \int_0^L M \kappa \, dx = \frac{1}{2} \int_0^L EI \kappa^2 \, dx = \frac{1}{2} \int_0^L EI (v'')^2 \, dx = \frac{1}{2} \int_0^L v'' EI v'' \, dx. \quad (12.7)$$

The external work  $W$  accounts for the applied transverse force:

$$W = \int_0^L q v \, dx. \quad (12.8)$$

The three functionals  $\Pi$ ,  $U$  and  $W$  must be regarded as depending on the transverse displacement  $v(x)$ . When this dependence needs to be emphasized we write  $\Pi[v]$ ,  $U[v]$  and  $W[v]$ .

Note that  $\Pi[v]$  includes up to second derivatives in  $v$ , because  $v'' = \kappa$  appears in  $U$ . This number is called the *variational index*. Variational calculus tells us that since the index is 2, admissible displacements  $v(x)$  must be continuous, have continuous first derivatives (slopes or rotations), and satisfy the displacement BCs exactly. This continuity requirement can be succinctly stated by saying that admissible displacements must be  $C^1$  continuous. This condition guides the construction of beam finite elements described below.

**Remark 12.1.** If there is an applied distributed moment  $m(x)$  per unit of beam length, the external energy (12.8) must be augmented with a  $\int_0^L m(x) \theta(x) \, dx$  term. This is further elaborated in Exercises 12.4 and 12.5. Such kind of distributed loading is uncommon in practice although in framework analysis occasionally the need arises for treating a concentrated moment between nodes.

### §12.5. Beam Finite Elements

Beam finite elements are obtained by subdividing beam members longitudinally. The simplest Bernoulli-Euler plane beam element has two end nodes: 1 and 2, and four degrees of freedom (DOF). These are collected in the node displacement vector

$$\mathbf{u}^e = [v_1 \ \theta_1 \ v_2 \ \theta_2]^T. \quad (12.9)$$

The element is shown in Figure 12.8, which pictures the undeformed and deformed configurations.

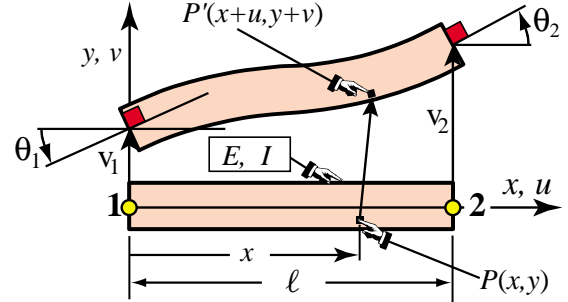


FIGURE 12.8. The two-node Bernoulli-Euler plane beam element with four DOFs.

#### §12.5.1. Finite Element Trial Functions

The freedoms (12.9) are used to define uniquely the variation of the transverse displacement  $v^e(x)$  over the element. The  $C^1$  continuity requirement says that both  $v(x)$  and the slope  $\theta = v'(x) = dv(x)/dx$  must be continuous over the entire member, and in particular between beam elements.

$C^1$  continuity can be trivially met *within each element* by choosing polynomial interpolation shape functions as shown below, because polynomials are  $C^\infty$  continuous. Matching nodal displacements and rotations with *adjacent elements* enforces the necessary interelement continuity.

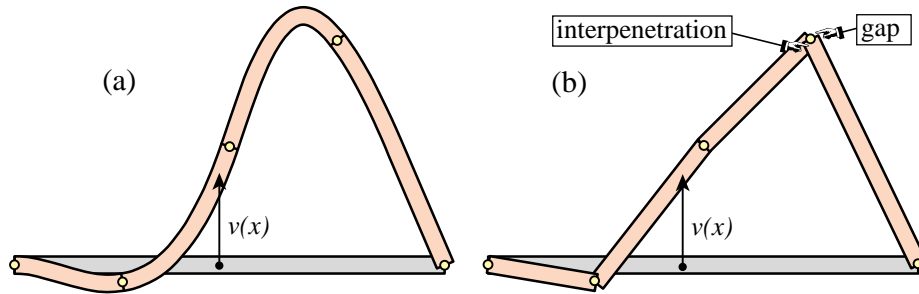


FIGURE 12.9. Deflection of a clamped-SS beam discretized with four elements, grossly exaggerated for visibility. (a) Cubic deflection elements; (b) linear deflection elements. The latter maintains only  $C^0$  continuity, leading to unacceptable material gap and interpenetration at nodes.

**Remark 12.2.** The physical reason for  $C^1$  continuity is illustrated in Figure 12.9, in which the lateral deflection curve  $v(x)$  is grossly exaggerated for visibility. The left figure shows the approximation of  $v(x)$  by four cubic functions, which maintain the required continuity. The right figure shows an attempt to approximate  $v(x)$  by four piecewise linear functions that maintain only  $C^0$  continuity. In this case material gap and interpenetration occur at the nodes, as well as at the clamped left end, because section rotations jump between elements.



## §12.5.2. Shape Functions

The simplest shape functions that meet the  $C^1$  continuity requirement for the nodal DOF configuration (12.9) are called the *Hermitian cubic* shape functions. The interpolation formula based on these functions is

$$v^e = [N_{v1}^e \ N_{\theta1}^e \ N_{v2}^e \ N_{\theta2}^e] \begin{bmatrix} v_1 \\ \theta_1 \\ v_2 \\ \theta_2 \end{bmatrix} = \mathbf{N}^e \mathbf{u}^e. \quad (12.10)$$

These shape functions are conveniently expressed in terms of the dimensionless “natural” coordinate

$$\xi = \frac{2x}{\ell} - 1, \quad (12.11)$$

where  $\ell$  is the element length. Coordinate  $\xi$  varies from  $\xi = -1$  at node 1 ( $x = 0$ ) to  $\xi = +1$  at node 2 ( $x = \ell$ ). Note that  $dx/d\xi = \frac{1}{2}\ell$  and  $d\xi/dx = 2/\ell$ . The shape functions in terms of  $\xi$  are

$$\begin{aligned} N_{v1}^e &= \frac{1}{4}(1 - \xi)^2(2 + \xi), \\ N_{\theta1}^e &= \frac{1}{8}\ell(1 - \xi)^2(1 + \xi), \\ N_{v2}^e &= \frac{1}{4}(1 + \xi)^2(2 - \xi), \\ N_{\theta2}^e &= -\frac{1}{8}\ell(1 + \xi)^2(1 - \xi). \end{aligned} \quad (12.12)$$

These four functions are depicted in Figure 12.10.

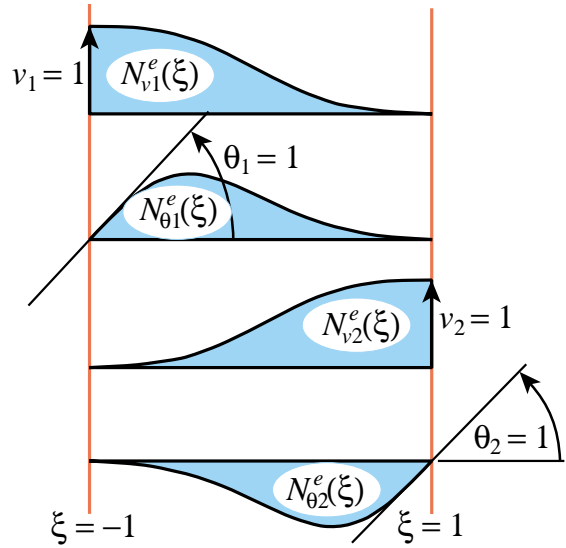


FIGURE 12.10. Cubic shape functions of plane beam element.

The curvature  $\kappa$  that appears in  $U$  can be expressed in terms of the nodal displacements by differentiating twice with respect to  $x$ :

$$\kappa = \frac{d^2 v^e(x)}{dx^2} = \frac{4}{\ell^2} \frac{d^2 v^e(\xi)}{d\xi^2} = \frac{4}{\ell^2} \frac{d\mathbf{N}^e}{d\xi^2} \mathbf{u}^e = \mathbf{B} \mathbf{u}^e = \mathbf{N}'' \mathbf{u}^e. \quad (12.13)$$

Here  $\mathbf{B} = \mathbf{N}''$  is the  $1 \times 4$  curvature-displacement matrix

$$\mathbf{B} = \frac{1}{\ell} \begin{bmatrix} 6\frac{\xi}{\ell} & 3\xi - 1 & -6\frac{\xi}{\ell} & 3\xi + 1 \end{bmatrix}. \quad (12.14)$$

**Remark 12.3.** The  $4/\ell^2$  factor in (12.13) comes from the differentiation chain rule. If  $f(x)$  is a function of  $x$ , and  $\xi = 2x/\ell - 1$ , noting that  $d(2/\ell)/dx = 0$  one gets

$$\frac{df(x)}{dx} = \frac{df(\xi)}{d\xi} \frac{d\xi}{dx} = \frac{2}{\ell} \frac{df(\xi)}{d\xi}, \quad \frac{d^2 f(x)}{dx^2} = \frac{d}{dx} \left( \frac{2}{\ell} \frac{df(\xi)}{d\xi} \right) = \frac{2}{\ell} \frac{d}{dx} \left( \frac{df(\xi)}{d\xi} \right) = \frac{4}{\ell^2} \frac{d^2 f(\xi)}{d\xi^2}. \quad (12.15)$$

```

ClearAll[EI,l,ξ];
Be={{6*ξ,(3*ξ-1)*l,-6*ξ,(3*ξ+1)*l}}/l^2;
Ke=(EI*l/2)*Integrate[Transpose[Be].Be,{ξ,-1,1}];
Ke=Simplify[Ke]; Print["Ke for prismatic beam:"];
Print[Ke//MatrixForm];
Print[Simplify[Ke*l^2/EI]//MatrixForm];

```

Ke for prismatic beam:

$$\begin{pmatrix} \frac{12EI}{l^3} & \frac{6EI}{l^2} & -\frac{12EI}{l^3} & \frac{6EI}{l^2} \\ \frac{6EI}{l^2} & \frac{4EI}{l} & -\frac{6EI}{l^2} & \frac{2EI}{l} \\ -\frac{12EI}{l^3} & -\frac{6EI}{l^2} & \frac{12EI}{l^3} & -\frac{6EI}{l^2} \\ \frac{6EI}{l^2} & \frac{2EI}{l} & -\frac{6EI}{l^2} & \frac{4EI}{l} \end{pmatrix}$$

FIGURE 12.11. Using *Mathematica* to form  $\mathbf{K}^e$  for a prismatic beam element.

```

ClearAll[q,l,ξ];
Ne={{2*(1-ξ)^2*(2+ξ), (1-ξ)^2*(1+ξ)*l,
      2*(1+ξ)^2*(2-ξ), -(1+ξ)^2*(1-ξ)*l}}/8;
fe=(q*l/2)*Integrate[Ne,{ξ,-1,1}]; fe=Simplify[fe];
Print["fe^T for uniform load q:\n",fe//MatrixForm];

```

fe^T for uniform load q:

$$\left( \frac{lq}{2} \quad \frac{l^2q}{12} \quad \frac{lq}{2} \quad -\frac{l^2q}{12} \right)$$

FIGURE 12.12. Using *Mathematica* to form  $\mathbf{f}^e$  for uniform transverse load  $q$ .

## §12.6. The Finite Element Equations

Insertion of (12.12) and (12.14) into the TPE functional specialized to this element, yields the quadratic form in the nodal displacements

$$\Pi^e = \frac{1}{2}(\mathbf{u}^e)^T \mathbf{K}^e \mathbf{u}^e - (\mathbf{u}^e)^T \mathbf{f}^e, \quad (12.16)$$

where

$$\mathbf{K}^e = \int_0^\ell EI \mathbf{B}^T \mathbf{B} dx = \int_{-1}^1 EI \mathbf{B}^T \mathbf{B} \frac{1}{2} \ell d\xi, \quad (12.17)$$

is the element stiffness matrix and

$$\mathbf{f}^e = \int_0^\ell \mathbf{N}^T q dx = \int_{-1}^1 \mathbf{N}^T q \frac{1}{2} \ell d\xi, \quad (12.18)$$

is the consistent element node force vector. The calculation of the entries of  $\mathbf{K}^e$  and  $\mathbf{f}^e$  for prismatic beams and uniform load  $q$  is studied next. More complex cases are treated in the Exercises.

### §12.6.1. The Stiffness Matrix of a Prismatic Beam

If the bending rigidity  $EI$  is constant over the element it can be moved out of the  $\xi$ -integral in (12.17):

$$\mathbf{K}^e = \frac{1}{2} EI \ell \int_{-1}^1 \mathbf{B}^T \mathbf{B} d\xi = \frac{EI}{2\ell} \int_{-1}^1 \begin{bmatrix} \frac{6\xi}{\ell} \\ 3\xi - 1 \\ -\frac{6\xi}{\ell} \\ 3\xi + 1 \end{bmatrix} \begin{bmatrix} \frac{6\xi}{\ell} & 3\xi - 1 & -\frac{6\xi}{\ell} & 3\xi + 1 \end{bmatrix} d\xi. \quad (12.19)$$

Expanding and integrating over the element yields

$$\mathbf{K}^e = \frac{EI}{2\ell^3} \int_{-1}^1 \begin{bmatrix} 36\xi^2 & 6\xi(3\xi-1)\ell & -36\xi^2 & 6\xi(3\xi+1)\ell \\ (3\xi-1)^2\ell^2 & -6\xi(3\xi-1)\ell & (9\xi^2-1)\ell^2 & 6\xi(3\xi+1)\ell \\ 36\xi^2 & -6\xi(3\xi+1)\ell & (3\xi+1)^2\ell^2 & 6\xi(3\xi-1)\ell \\ \text{symm} & & & \end{bmatrix} d\xi = \frac{EI}{\ell^3} \begin{bmatrix} 12 & 6\ell & -12 & 6\ell \\ & 4\ell^2 & -6\ell & 2\ell^2 \\ & & 12 & -6\ell \\ \text{symm} & & & 4\ell^2 \end{bmatrix} \quad (12.20)$$

Although the foregoing integrals can be easily carried out by hand, it is equally expedient to use a CAS such as *Mathematica* or *Maple*. For example the *Mathematica* script listed in the top box of Figure 12.11 processes (12.20) using the *Integrate* function. The output, shown in the bottom box, corroborates the hand integration result.

### §12.6.2. Consistent Nodal Force Vector for Uniform Load

If  $q$  does not depend on  $x$  it can be moved out of (12.18), giving

$$\mathbf{f}^e = \frac{1}{2}q\ell \int_{-1}^1 \mathbf{N}^T d\xi = \frac{1}{2}q\ell \int_{-1}^1 \begin{bmatrix} \frac{1}{4}(1-\xi)^2(2+\xi) \\ \frac{1}{8}\ell(1-\xi)^2(1+\xi) \\ \frac{1}{4}(1+\xi)^2(2-\xi) \\ -\frac{1}{8}\ell(1+\xi)^2(1-\xi) \end{bmatrix} d\xi = \frac{1}{2}q\ell \begin{bmatrix} 1 \\ \frac{1}{6}\ell \\ 1 \\ -\frac{1}{6}\ell \end{bmatrix}. \quad (12.21)$$

This shows that a uniform load  $q$  over the beam element maps to two transverse node loads  $q\ell/2$ , as may be expected, plus two nodal moments  $\pm q\ell^2/12$ . The latter are called the *fixed-end moments* in the structural mechanics literature.<sup>3</sup> The hand result (12.21) can be verified with the *Mathematica* script of Figure 12.12, in which  $\mathbf{f}^e$  is printed as a row vector to save space.

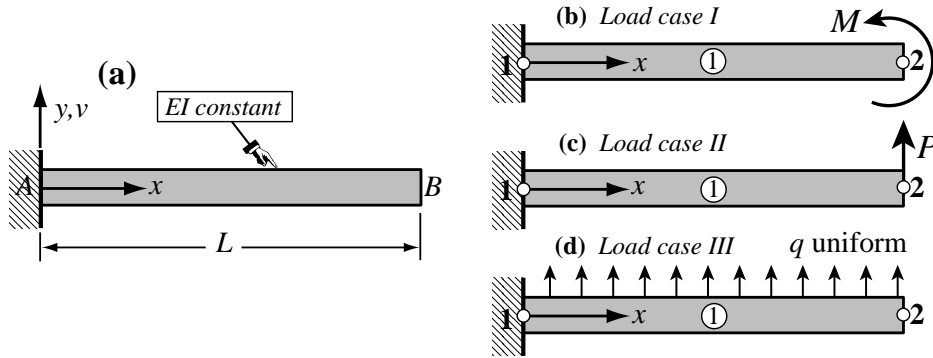


FIGURE 12.13. Cantilever beam problem for Example 12.1: (a) structure, (b-c): one-element FEM idealizations for three load cases.

**Example 12.1.** To see the beam element in action consider the cantilever illustrated in Figure 12.13(a). The beam is prismatic with constant rigidity  $EI$  and span  $L$ . It is discretized with a single element as shown in Figure 12.13(b,c,d), and subjected to the three load cases pictured there. Case I involves an applied end moment  $M$ , case II a transverse end force  $P$ , and case III a uniformly distributed load  $q$  over the entire beam. The FEM equations are constructed using the stiffness matrix (12.20) with  $\ell = L$ .

For the first two load cases, forces at end node 2 are directly set up from the given loads since no lumping is needed. Applying the support conditions  $v_1 = \theta_1 = 0$  gives the reduced stiffness equations

$$\frac{EI}{L^3} \begin{bmatrix} 12 & -6L \\ -6L & 4L^2 \end{bmatrix} \begin{bmatrix} v_2^I \\ \theta_2^I \end{bmatrix} = \begin{bmatrix} 0 \\ M \end{bmatrix}, \quad \frac{EI}{L^3} \begin{bmatrix} 12 & -6L \\ -6L & 4L^2 \end{bmatrix} \begin{bmatrix} v_2^{II} \\ \theta_2^{II} \end{bmatrix} = \begin{bmatrix} P \\ 0 \end{bmatrix}, \quad (12.22)$$

<sup>3</sup> Introduced by Hardy Cross in 1930 (long before FEM) as a key ingredient for his moment distribution method. Indeed the title of his famous paper [174] is “Analysis of continuous frames by distributing fixed-end moments.”

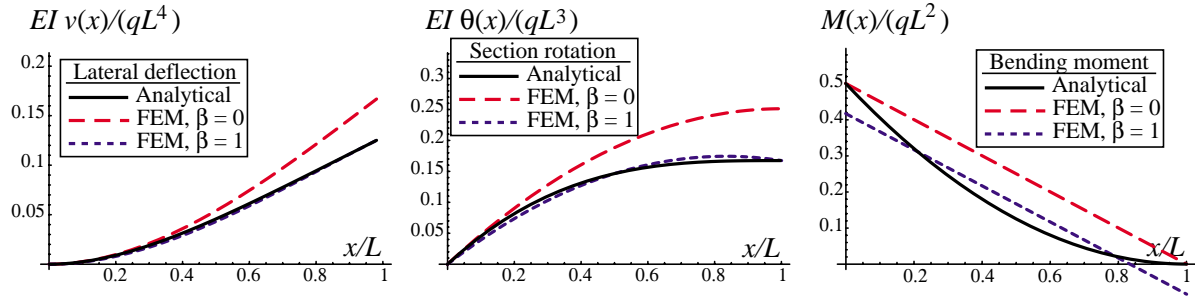


FIGURE 12.14. FEM versus analytical solutions for load case III of Example 12.1.

for load cases I and II, respectively. Solving gives the tip deflections  $v_2^I = ML^2/(2EI)$  and  $v_2^{II} = PL^3/(3EI)$ , and the tip rotations  $\theta_2^I = ML/EI$  and  $\theta_2^{II} = PL^2/(2EI)$ . These agree with the analytical values provided by Bernoulli-Euler beam theory. Thus a one-element idealization is sufficient for exactness. The reason is that the analytical deflection profiles  $v(x)$  are quadratic and cubic polynomials in  $x$  for cases I and II, respectively. Both are included in the span of the element shape functions. Displacements  $v(x)$ , rotations  $\theta(x)$  and moments  $M(x)$  expressed as functions of  $x$  also agree with the analytical solution, as may be expected.

The results for load case III are more interesting since now the exact deflection is a quartic polynomial, which lies beyond the span of the FEM shape functions. A dimensionless parameter  $0 \leq \beta \leq 1$  is introduced in the reduced stiffness equations to study the effect of load lumping method on the solution:

$$\frac{EI}{L^3} \begin{bmatrix} 12 & -6L \\ -6L & 4L^2 \end{bmatrix} \begin{bmatrix} v_2^{III} \\ \theta_2^{III} \end{bmatrix} = \frac{1}{2} q L \begin{bmatrix} 1 \\ -\frac{1}{6}\beta L \end{bmatrix}. \quad (12.23)$$

Setting  $\beta = 1$  gives the energy consistent load lumping (12.21) whereas  $\beta = 0$  gives the EbE (here same as NbN) load lumping  $f_2^{III} = \frac{1}{2} q L$  with zero fixed-end moments. The solution of (12.23) is  $v_2^{III} = q L^4(4 - \beta)/(24 EI)$  and  $\theta_2^{III} = q L^3(3 - \beta)/(12 EI)$ . From this one recovers the displacement, rotation and bending moment over the beam as

$$v^{III}(x) = q L^2 x^2 \frac{L(6-\beta) - 2x}{24 EI}, \quad \theta^{III}(x) = q L x \frac{L(6-\beta) - 3x}{12 EI}, \quad M^{III}(x) = \frac{q L}{12} (L(6-\beta) - 6x). \quad (12.24)$$

The analytical (exact) solution is

$$v_{ex}^{III}(x) = \frac{q x^2(3L^2 - 3Lx + x^2)}{24 EI}, \quad \theta_{ex}^{III}(x) = \frac{q x(6L^2 - 4Lx + x^2)}{6 EI}, \quad M_{ex}^{III}(x) = \frac{1}{2} q (L - x)^2. \quad (12.25)$$

The FEM and analytical solutions (12.24)-(12.25) are graphically compared in Figure 12.14. Deflections and rotations obtained with the consistent load lumping  $\beta = 1$  agree better with the analytical solution. In addition the nodal values are exact (a superconvergence result further commented upon in the next Example). For the bending moment the values provided by the EbE lumping  $\beta = 0$  are nodally exact but over the entire beam the  $\beta = 1$  solution gives a better linear fit to the parabolic function  $M_{ex}^{III}(x)$ .

**Example 12.2.** The second example involves a simply supported beam under uniform line load  $q$ , depicted in Figure 12.15(a). It is prismatic with constant rigidity  $EI$ , span  $L$ , and discretized with two elements of length  $L_1 = L(1/2 + \alpha)$  and  $L_2 = L - L_1 = L(1/2 - \alpha)$ , respectively. (Ordinarily two elements of the same length  $1/2L$  would be used; the scalar  $\alpha \in (-1/2, 1/2)$  is introduced to study the effect of unequal element sizes.)

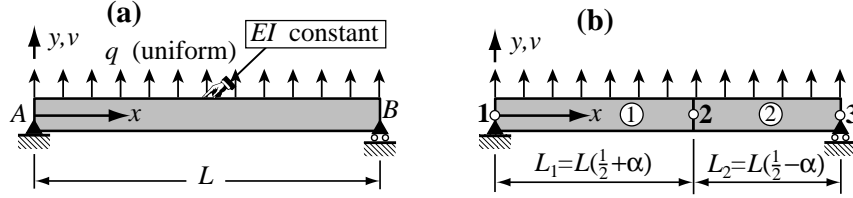


FIGURE 12.15. SS beam problem for Example 12.2: (a) structure, (b) two-element FEM idealization.

Using (12.20) and (12.21) to form the stiffness and consistent forces for both elements, assembling and applying the support conditions  $v_1 = v_3 = 0$ , provides the reduced stiffness equations

$$\frac{EI}{L^3} \begin{bmatrix} \frac{8L^2}{1+2\alpha} & \frac{-24L}{(1+2\alpha)^2} & \frac{4L^2}{1+2\alpha} & 0 \\ \frac{-24L}{(1+2\alpha)^2} & \frac{192(1+12\alpha^2)}{(1-4\alpha^2)^3} & \frac{192L\alpha}{(1-4\alpha^2)^2} & \frac{24L}{(1-2\alpha)^2} \\ \frac{4L^2}{1+2\alpha} & \frac{192L\alpha}{(1-4\alpha^2)^2} & \frac{16L^2}{1-4\alpha^2} & \frac{4L^2}{1-2\alpha} \\ 0 & \frac{24L}{(1-2\alpha)^2} & \frac{4L^2}{1-2\alpha} & \frac{8L^2}{1-2\alpha} \end{bmatrix} \begin{bmatrix} \theta_1 \\ v_2 \\ \theta_2 \\ \theta_3 \end{bmatrix} = \frac{qL}{2} \begin{bmatrix} \frac{L(1+2\alpha)^2}{24} \\ 1 \\ -\frac{L\alpha}{3} \\ -\frac{L(1-2\alpha)^2}{24} \end{bmatrix}. \quad (12.26)$$

Solving for the lateral displacement of node 2 gives  $v_2 = qL^4(5 - 24\alpha^2 + 16\alpha^4)/(384EI)$ . The exact deflection is  $v(x) = qL^4(\zeta - 2\zeta^3 + \zeta^4)/(24EI)$  with  $\zeta = x/L$ . Replacing  $x = L_1 = L(1/2 + \alpha)$  yields  $v_2^{exact} = qL^4(5 - 24\alpha^2 + 16\alpha^4)/(384EI)$ , which is the same as the FEM result. Likewise  $\theta_2$  is exact.

The result seems *prima facie* surprising. First, since the analytical solution is a quartic polynomial in  $x$  we have no reason to think that a cubic element will be exact. Second, one would expect accuracy deterioration as the element sizes differ more and more with increasing  $\alpha$ . The fact that the solution at nodes is exact for any combination of element lengths is an illustration of *superconvergence*, a phenomenon already discussed in §11.5. A general proof of nodal exactness is given in §13.7, but it does require advanced mathematical tools. Note that displacements and rotations *inside* elements will not agree with the exact one; this can be observed in Figure 12.14(a,b) for load case III of the previous example.

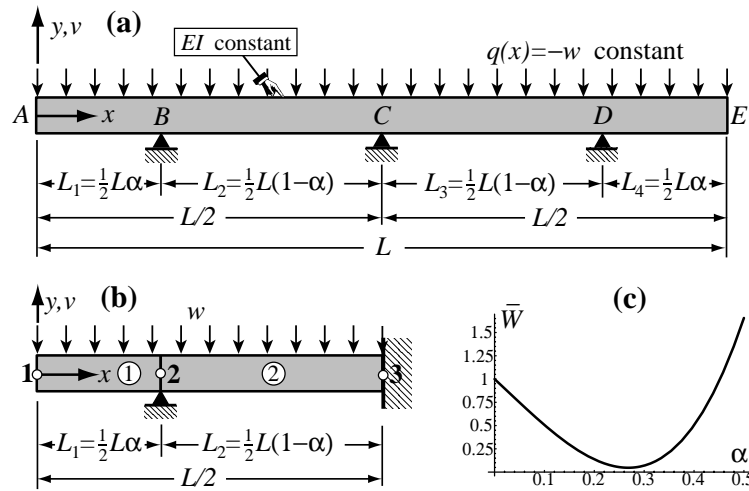


FIGURE 12.16. Continuum beam problem for Example 12.3, (a): structure, (b) two-element FEM model of half beam, (c) scaled external energy of FEM model as function of  $\alpha$ .

**Example 12.3.** (Adapted from a driven-tank experiment by Patrick Weidman). This example displays the advantages of symbolic computation for solving a problem in geometric design: optimal location of supports. The prismatic continuous beam shown in Figure 12.16(a) is free at ends A and E, and simply supported at B, C and D. The beam has total span  $L$  and constant bending rigidity  $EI$ . It is loaded by a uniform distributed load  $q(x) = -w$ . Support C is at midspan whereas B and D are at distances  $L_1 = L_4 = \frac{1}{2}L\alpha$  from the left and right free ends, respectively. Here  $0 \leq \alpha < 1$  is a design parameter to be determined as discussed later.

Since the problem is symmetric about midspan C only one half of the structure, say AC, need to be discretized. The finite element model of this portion is shown in Figure 12.16(b). It has two beam elements and three nodes placed at A, B and C, respectively. Element lengths depend on the design parameter  $\alpha$ , which is carried along as a variable. The six degrees of freedom are collected in  $\mathbf{u} = [v_1 \ \theta_1 \ v_2 \ \theta_2 \ v_3 \ \theta_3]^T$ . The master stiffness equations are

$$\frac{4EI}{L^3} \begin{bmatrix} \frac{24}{\alpha^3} & \frac{6L}{\alpha^2} & -\frac{24}{\alpha^3} & \frac{6L}{\alpha^2} & 0 & 0 \\ \frac{6L}{\alpha^2} & \frac{2L^2}{\alpha} & -\frac{6L}{\alpha^2} & \frac{L^2}{\alpha} & 0 & 0 \\ -\frac{24}{\alpha^3} & -\frac{6L}{\alpha^2} & \frac{24(1-3\alpha\hat{\alpha})}{\alpha^3\hat{\alpha}^3} & -\frac{6L(1-2\alpha)}{\alpha^2\hat{\alpha}^2} & -\frac{24}{\hat{\alpha}^3} & \frac{6L}{\hat{\alpha}^2} \\ \frac{6L}{\alpha^2} & \frac{L^2}{\alpha} & -\frac{6L(1-2\alpha)}{\alpha^2\hat{\alpha}^2} & \frac{2L^2}{\alpha\hat{\alpha}} & -\frac{6L}{\hat{\alpha}^2} & \frac{L^2}{\hat{\alpha}} \\ 0 & 0 & -\frac{24}{\hat{\alpha}^3} & -\frac{6L}{\hat{\alpha}^2} & \frac{24}{\hat{\alpha}^3} & -\frac{6L}{\hat{\alpha}^2} \\ 0 & 0 & \frac{6L}{\hat{\alpha}^2} & \frac{L^2}{\hat{\alpha}} & -\frac{6L}{\hat{\alpha}^2} & \frac{2L^2}{\hat{\alpha}} \end{bmatrix} \begin{bmatrix} v_1 \\ \theta_1 \\ v_2 \\ \theta_2 \\ v_3 \\ \theta_3 \end{bmatrix} = \frac{wL}{4} \begin{bmatrix} -\alpha \\ -\frac{L\alpha^2}{12} \\ -1 \\ \frac{L(2\alpha-1)}{12} \\ -\hat{\alpha} \\ \frac{L\hat{\alpha}^2}{12} \end{bmatrix} + \begin{bmatrix} 0 \\ 0 \\ f_2^r \\ 0 \\ f_3^r \\ m_3^r \end{bmatrix} \quad (12.27)$$

in which  $\hat{\alpha} = 1 - \alpha$ . Note that reaction forces are carefully segregated in (12.27) to simplify application of the general recovery technique discussed in §3.4.3. The support BCs are  $v_2 = v_3 = \theta_3 = 0$ , where the latter comes from the symmetry condition at C. Removing those freedoms provides the reduced stiffness equations

$$\frac{4EI}{L^3} \begin{bmatrix} \frac{24}{\alpha^3} & \frac{6L}{\alpha^2} & \frac{6L}{\alpha^2} \\ \frac{6L}{\alpha^2} & \frac{2L^2}{\alpha} & \frac{L^2}{\alpha} \\ \frac{6L}{\alpha^2} & \frac{L^2}{\alpha} & \frac{2L^2}{\alpha\hat{\alpha}} \end{bmatrix} \begin{bmatrix} v_1 \\ \theta_1 \\ \theta_2 \end{bmatrix} = \frac{wL}{4} \begin{bmatrix} -\alpha \\ -\frac{L\alpha^2}{12} \\ \frac{L(2\alpha-1)}{12} \end{bmatrix}. \quad (12.28)$$

Solving yields

$$v_1 = -\frac{wL^4}{768EI} \alpha ((1+\alpha)^3 - 2), \quad \theta_1 = \frac{wL^3}{384EI} ((1+\alpha)^3 - 2), \quad \theta_2 = \frac{wL^3}{384EI} \hat{\alpha} (1 - 2\alpha - 5\alpha^2). \quad (12.29)$$

The complete solution is  $\mathbf{u} = [v_1 \ \theta_1 \ 0 \ \theta_2 \ 0 \ 0]^T$ . Inserting into (12.27) and solving for reactions gives

$$f_{r2} = \frac{wL}{16} \frac{3 + 2\alpha + \alpha^2}{\hat{\alpha}}, \quad f_{r3} = \frac{wL}{16} \frac{5 - 10\alpha - \alpha^2}{\hat{\alpha}}, \quad m_{r3} = -\frac{wL^2}{32} (1 - 2\alpha - \alpha^2). \quad (12.30)$$

whence the support reactions follow as  $R_B = f_{r2}$  and  $R_C = 2f_{r3}$ . It remains to find the best  $\alpha$ . Of course “best” depends on the optimality criterion. Four choices are examined below.

**Minimum External Energy.** The external energy at equilibrium is  $W(\alpha) = \mathbf{f}^T \mathbf{u} = w^2 L^5 \bar{W}(\alpha) / (18432 EI)$ , in which  $\bar{W}(\alpha) = 1 - 5\alpha - 2\alpha^2 + 26\alpha^3 + 5\alpha^4 + 3\alpha^5$ . Minimizing  $W$  with respect to  $\alpha$  may be interpreted as finding the stiffest structure (in the energy sense) under the given load vector  $\mathbf{f}$ . A plot of  $\bar{W}(\alpha)$  over  $0 \leq \alpha \leq \frac{1}{2}$  clearly displays a minimum at  $\alpha \approx 0.27$  as shown in Figure 12.16(c). Solving the quartic equation  $d\bar{W}/d\alpha = 0$  gives one positive real root in the range  $\alpha \in [0, 1)$ , which to 5 places is  $\alpha_{best} = 0.26817$ .

*Equal Reactions.* A second choice is to require that supports at B and C take the same load:  $R_B = R_C$  (note that, because of symmetry,  $R_D = R_B$ ). Setting  $f_{r2} = 2f_{r3}$  with their expressions taken from (12.30), yields  $3 + 2\alpha + \alpha^2 = 10 - 20\alpha - 2\alpha^2$ , or  $7 - 22\alpha - 3\alpha^2 = 0$ . This quadratic has the roots  $\alpha = \frac{1}{3}(-11 \pm \sqrt{142})$ . The positive real root  $\alpha_{best} = 0.30546$  makes  $R_B = R_C = R_D = wL/3$ , as may be expected.

*Minimum Relative Deflection.* Consider two sections located at  $x_i$  and  $x_j$ , in which  $\{x_i, x_j\} \in [0, \frac{1}{2}L]$ , with lateral displacements  $v_i = v(x_i)$  and  $v_j = v(x_j)$ , respectively. The maximum relative deflection is defined as  $v_{ji}^{max}(\alpha) = \max |v_j - v_i|$  for a fixed  $\alpha$ . We seek the  $\alpha \in [0, 1)$  that minimizes  $v_{ji}^{max}(\alpha)$ . The computations are far more complex than for the previous two criteria and are the subject of Exercise 12.11. Result: the best  $\alpha$  is the positive real root of  $4 + 11\alpha - 81\alpha^2 - 49\alpha^3 - 47\alpha^4 = 0$ , which to 5 places is  $\alpha_{best} = 0.26681$ . If this value is adopted, the relative deflection does not exceed  $v_{ij}^{max} < wL^4/(67674EI)$ .

*Minimum Absolute Moment.* Let  $M(x, \alpha)$  denote the bending moment function recovered from the FEM solution for a fixed  $\alpha$ . The maximum absolute moment is  $M^{max}(\alpha) = \max |M(x, \alpha)|$  for  $x \in [0, \frac{1}{2}L]$ . We seek an  $\alpha \in [0, 1)$  that minimizes it. This is the topic of Exercise 12.12. This problem is less well posed than the previous one because  $M(x, \alpha)$  varies linearly over each element, is nonzero at node 1 and discontinuous at node 2. On the other hand, the exact bending moment varies parabolically, is zero at node 1 and continuous at node 2. Result: using the FEM-recovered  $M(x, \alpha)$  and taking the average  $M$  at node 2, one finds that the best  $\alpha$  is the positive root of  $2 - 4\alpha - 15\alpha^2 = 0$ , or  $\alpha_{best} = 0.25540$ , for which  $M^{max} < wL^2/589$ . The optimal solution using the exact moment distribution, however, is quite different. This is an intrinsic weakness of displacement-based FEM since internal forces are obtained by differentiation, which boosts errors. To get a better result a finer mesh would be needed.

In summary, the optimal  $\alpha$  from the foregoing criteria varies between 0.255 to 0.306. As a reasonable compromise an engineer could pick  $\alpha_{best} \approx 0.28$ .

## Notes and Bibliography

The Bernoulli-Euler (BE) beam model synthesizes pioneer work by Jacob and Daniel Bernoulli as well as that of Leonhard Euler in the XVIII Century. Although the model was first enunciated by 1750, it was not applied in structural design and analysis until the second half of the XIX Century. While Galileo Galilei is credited with first attempts at a theory, recent studies [43] argue that Leonardo da Vinci made crucial observations a century before Galileo. However, da Vinci lacked Hooke's law and calculus to complete the theory.

A comprehensive source of stiffness and mass matrices of plane and spatial beams is the book by Przemieniecki [603]. The derivation of stiffness matrices is carried out there using differential equilibrium equations rather than energy methods. This was in fact the common practice before 1962, as influenced by the use of transfer matrix methods [578] on the limited memory computers of the time. Results for prismatic elements, however, are identical.

Energy derivations were popularized by Archer [35,36], Martin [473] and Melosh [490,491].

## References

Referenced items have been moved to Appendix R.

### Homework Exercises for Chapter 12

#### Variational Formulation of Plane Beam Element

**EXERCISE 12.1** [A/C:20] Use (12.17) to derive the element stiffness matrix  $\mathbf{K}^e$  of a Hermitian beam element of variable bending rigidity given by the inertia law

$$I(x) = I_1(1 - \frac{x}{\ell}) + I_2 \frac{x}{\ell} = I_1 \frac{1}{2}(1 - \xi) + I_2 \frac{1}{2}(1 + \xi). \quad (\text{E12.1})$$

Use of *Mathematica* or similar CAS tool is recommended since the integrals are time consuming and error prone. *Mathematica* hint: write

$$\text{EI} = \text{EI1}*(1-\xi)/2 + \text{EI2}*(1+\xi)/2; \quad (\text{E12.2})$$

and keep EI inside the argument of `Integrate`. Check whether you get back (12.20) if  $\text{EI}=\text{EI1}=\text{EI2}$ . If you use *Mathematica*, this check can be simply done after you got and printed the tapered beam  $\mathbf{K}^e$ , by writing `ClearAll[EI]; Ke=Simplify[ Ke/.{EI1->EI,EI2->EI}];` and printing this matrix.<sup>4</sup>

**EXERCISE 12.2** [A/C:20] Use (12.18) to derive the consistent node force vector  $\mathbf{f}^e$  for a Hermitian beam element under linearly varying transverse load  $q$  defined by

$$q(x) = q_1(1 - \frac{x}{\ell}) + q_2 \frac{x}{\ell} = q_1 \frac{1}{2}(1 - \xi) + q_2 \frac{1}{2}(1 + \xi). \quad (\text{E12.3})$$

Again use of a CAS is recommended, particularly since the polynomials to be integrated are quartic in  $\xi$ , and hand computations are error prone. *Mathematica* hint: write

$$q = q1*(1-\xi)/2 + q2*(1+\xi)/2; \quad (\text{E12.4})$$

and keep  $q$  inside the argument of `Integrate`. Check whether you get back (12.21) if  $q_1 = q_2 = q$  (See previous Exercise for *Mathematica* procedural hints).

**EXERCISE 12.3** [A:20] Obtain the consistent node force vector  $\mathbf{f}^e$  of a Hermitian beam element subject to a transverse point load  $P$  at abscissa  $x = a$  where  $0 \leq a \leq \ell$ . Use the Dirac's delta function expression  $q(x) = P \delta(a)$  and the fact that for any continuous function  $f(x)$ ,  $\int_0^\ell f(x) \delta(a) dx = f(a)$  if  $0 \leq a \leq \ell$ . Check the special cases  $a = 0$  and  $a = \ell$ .

**EXERCISE 12.4** [A:25] Derive the consistent node force vector  $\mathbf{f}^e$  of a Hermitian beam element subject to a linearly varying  $z$ -moment  $m$  per unit length, positive CCW, defined by the law  $m(x) = m_1(1 - \xi)/2 + m_2(1 + \xi)/2$ . Use the fact that the external work per unit length is  $m(x)\theta(x) = m(x) v'(x) = (\mathbf{u}^e)^T (d\mathbf{N}/dx)^T m(x)$ . For arbitrary  $m(x)$  show that this gives

$$\mathbf{f}^e = \int_0^\ell \frac{\partial \mathbf{N}^T}{\partial x} m dx = \int_{-1}^1 \frac{\partial \mathbf{N}^T}{\partial \xi} \frac{2}{\ell} m \frac{1}{2} \ell d\xi = \int_{-1}^1 \mathbf{N}_\xi^T m d\xi, \quad (\text{E12.5})$$

where  $\mathbf{N}_\xi^T$  denote the column vectors of beam shape function derivatives with respect to  $\xi$ . Can you see a shortcut that avoids the integral altogether if  $m$  is constant?

**EXERCISE 12.5** [A:20] Obtain the consistent node force vector  $\mathbf{f}^e$  of a Hermitian beam element subject to a concentrated moment ("point moment", positive CCW)  $C$  applied at  $x = a$ . Use the Concentrated moment load on beam element expression (E12.5) in which  $m(x) = C \delta(a)$ , where  $\delta(a)$  denotes the Dirac's delta function at  $x = a$ . Check the special cases  $a = 0$ ,  $a = \ell$  and  $a = \ell/2$ .

<sup>4</sup> `ClearAll[EI]` discards the previous definition (E12.2) of EI; the same effect can be achieved by writing `EI=. (dot)`.



**EXERCISE 12.6** [A/C:25] Consider the one-dimensional Gauss integration rules.<sup>5</sup>

$$\text{One point : } \int_{-1}^1 f(\xi) d\xi \doteq 2f(0). \quad (\text{E12.6})$$

$$\text{Two points: } \int_{-1}^1 f(\xi) d\xi \doteq f(-1/\sqrt{3}) + f(1/\sqrt{3}). \quad (\text{E12.7})$$

$$\text{Three points: } \int_{-1}^1 f(\xi) d\xi \doteq \frac{5}{9}f(-\sqrt{3/5}) + \frac{8}{9}f(0) + \frac{5}{9}f(\sqrt{3/5}). \quad (\text{E12.8})$$

Try each rule on the monomial integrals

$$\int_{-1}^1 d\xi, \quad \int_{-1}^1 \xi d\xi, \quad \int_{-1}^1 \xi^2 d\xi, \quad \dots \quad (\text{E12.9})$$

until the rule fails. In this way verify that rules (E12.6), (E12.7) and (E12.8) are exact for polynomials of degree up to 1, 3 and 5, respectively. (*Labor-saving hint*: for odd monomial degree no computations need to be done; why?).

**EXERCISE 12.7** [A/C:25] Repeat the derivation of Exercise 12.1 using the two-point Gauss rule (E12.7) to evaluate integrals in  $\xi$ . A CAS is recommended. If using *Mathematica* you may use a function definition to save typing. For example to evaluate  $\int_{-1}^1 f(\xi) d\xi$  in which  $f(\xi) = 6\xi^4 - 3\xi^2 + 7$ , by the 3-point Gauss rule (E12.8), say

```
f[ξ_]:=6ξ^4-3ξ^2+7; int=Simplify[(5/9)*(f[-Sqrt[3/5]]+f[Sqrt[3/5]])+(8/9)*f[0]];
```

and print `int`. To form an element by Gauss integration define matrix functions in terms of  $\xi$ , for example `Be[ξ_]`, or use the substitution operator `/.`, whatever you prefer. Check whether one obtains the same answers as with analytical integration, and explain why there is agreement or disagreement. Hint for the explanation: consider the order of the  $\xi$  polynomials you are integrating over the element.

**EXERCISE 12.8** [A/C:25] As above but for Exercise 12.2.

**EXERCISE 12.9** [A/C:30] Derive the Bernoulli-Euler beam stiffness matrix (12.20) using the method of differential equations. To do this integrate the homogeneous differential equation  $EI v'''' = 0$  four times over a cantilever beam clamped at node 1 over  $x \in [0, \ell]$  to get  $v(x)$ . The process yields four constants of integration  $C_1$  through  $C_4$ , which are determined by matching the two zero-displacement BCs at node 1 and the two force BCs at node 2. This provides a  $2 \times 2$  flexibility matrix relating forces and displacements at node  $j$ . Invert to get a deformational stiffness, and expand to  $4 \times 4$  by letting node 1 translate and rotate.

**EXERCISE 12.10** [C:20] Using *Mathematica*, repeat Example 12.2 but using EbE lumping of the distributed force  $q$ . (It is sufficient to set the nodal moments on the RHS of (12.26) to zero.) Is  $v_2$  the same as the exact analytical solution? If not, study the ratio  $v_2/v_2^{exact}$  as function of  $\alpha$ , and draw conclusions.

**EXERCISE 12.11** [C:25] For the continuous beam of Example 12.3, verify the results given there for the optimal  $\alpha$  that minimizes the maximum relative deflection. Plot the deflection profile when  $\alpha = \alpha_{best}$ .

**EXERCISE 12.12** [C:25] For the continuous beam of Example 12.3, verify the results given there for the optimal  $\alpha$  that minimizes the absolute bending moment. Plot the moment diagram when  $\alpha = \alpha_{best}$ .

---

<sup>5</sup> Gauss integration is studied further in Chapter 17.